Automatically Create Digital Elevation Model from Photos Captured by a Low-Cost UAV-Based System

Nguyen, Kiet Tuan; Phan, Anh Thu Thi; Truong-Hong, Linh

Citation (APA)
Nguyen, K. T., Phan, A. T. T., & Truong-Hong, L. (2023). Automatically Create Digital Elevation Model from Photos Captured by a Low-Cost UAV-Based System. In J. N. Reddy, C. M. Wang, V. H. Luong, & A. T. Le (Eds.), *Proceedings of the 3rd International Conference on Sustainable Civil Engineering and Architecture - ICSCEA 2023: ICSCEA 2023, 19–21 July, Da Nang City, Vietnam* (pp. 1633-1641). (Lecture Notes in Civil Engineering; Vol. 442). Springer. https://doi.org/10.1007/978-981-99-7434-4_176

Important note
To cite this publication, please use the final published version (if applicable).
Please check the document version above.

Automatically Create Digital Elevation Model from Photos Captured by a Low-Cost UAV-Based System

Kiet Tuan Nguyen[1,2], Anh Thu Thi Phan[1,2(✉)], and Linh Truong-Hong[3]

[1] Faculty of Civil Engineering, Ho Chi Minh City University of Technology (HCMUT), 268 Ly Thuong Kiet Street, District 10, Ho Chi Minh City, Vietnam
ptathu@hcmut.edu.vn

[2] Vietnam National University Ho Chi Minh City, Linh Trung Ward, Thu Duc District, Ho Chi Minh City, Vietnam

[3] Faculty of Civil Engineering and Geoscience, Delft University of Technology (TU Delft), Building 23, Stevinweg 1, 2628. CN Delft, Netherlands

Abstract. Unmanned aerial vehicles (UAVs) are commonly utilized as cost-effective devices for data collection by capturing photos of target objects. UAV images have been used for many applications, such as civil engineering, transportation, architecture, surveying, and mapping. Although commercial UAV image data processing software is suitable for generating orthoimages and dense point clouds of surfaces, it still requires extensive labor to prepare the appropriate point cloud to create a digital elevation model (DEM). This study proposes a method to automatically create DEM from a point cloud generated from UAV images. The proposed method composes of three main steps: (1) Candidate ground points, (2) Ground points extraction, and (3) Creation of a DEM model. The proposed method was tested on three datasets, covering a total area of approximately 45 hectares from 200 images captured by DJI Phantom 4 drone. As a result, the DEMs are successfully created with a spatial resolution of 1.0 m.

Keywords: UAV Photogrammetry · Unmanned Aerial Vehicles · Digital Elevation Models · Structure from Motion

1 Introduction

The digital elevation model (DEM) provides detailed and visually appealing information about the terrain, which has extensive applications in resource management, terrain mapping, urban planning, and disaster response [1–3]. Traditional methods of collecting elevation data for creating DEM involve topographic surveying and generating 3D points from stereo pair images captured by piloted aircraft systems. These methods require direct measurement and consume significant time and effort. Moreover, the quality of manual measurement was subjected to the technician's experience.

With the rapid development of unmanned aerial vehicles (UAV), these units acquire aerial images faster than traditional methods at a low cost while still providing the necessary elevation data with acceptable accuracy. Moreover, the high-resolution imagery in several centimeters captured by UAVs facilitates the generation of dense point clouds on the surface [4], accurately representing the surveyed terrain. Then, DEM can be generated from these point clouds.

Various methods have been applied for extracting ground points from point clouds, such as Cloth Simulation Filtering (CSF) [5], Multiscale Curvature Classification (MCC) [6], Progressive TIN based [7], Surface-based filtering [8], and Deep Convolutional Neural Networks [9]. However, these methods still exhibit classification errors and give incorrect classification, which causes an error in generating DEM. Moreover, commercial software has challenges in accurately classifying and extracting ground points from raster images.

This study presents the method of generating DEMs from UAV imagery. Ground points are extracted from the generated point cloud and subsequently created DEM. In this implementation, Kernel Density Estimation (KDE) [10] and Principal Component Analysis (PCA) [11] were used to extract potential point clouds of the ground, while Region Growing based cell was employed to group ground points. The outliers of the extracted ground points are filtered using the Radius Outlier Removal algorithm [13] to eliminate misclassified and erroneous samples. Finally, the Delaunay triangulation algorithm is utilized to create DEM.

Fig. 1. The point cloud data was used in this study. **a** Test site 1, **b** test site 2, and **c** test site 3

2   Study Area and Data Pre-processing

This study area includes two different areas captured using a DJI Phantom 4 RTK device with a DJI FC6310R camera, consisting of 110 images for Area 1 and 89 for Area 2. Subsequently, Agisoft Metashape software was used to generate point clouds. Area 1 was divided into two datasets, while one was for Area 2. Dataset 1 (Test site 1) combines bare soil and existing construction, Dataset 2 (Test site 2) is mainly covered by existing construction, and Dataset 3 (Test site 3) is almost bare soil (Fig. 1). Table 1 shows the general information of the three datasets including the number of 3D points and test site dimension.

Table 1. The information of three test sites

	Test 1	Test 2	Test 3
Points	46 538 636	43 941 595	56 860 434
Dimensions (m)	450 × 450	430 × 430	250 × 250

Table 2. The parameters used for data processing

	Step 1			Step 2			Step 3		
Parameters	Test 1	Test 2	Test 3	Test 1	Test 2	Test 3	Test 1	Test 2	Test 3
Cell size(m)	25.0	55	5	2.0	2.0	2.0	1.0	1.0	1.0
Bandwidth (m)	0.65	0.8	0.5	–	–	–	–	–	–
Range numlocs	0.05	0.05	0.05	–	–	–	–	–	–
f	–	–	–	0.15	0.1	0.1	–	–	–
T(m)	–	–	–	0.15	0.15	0.15	–	–	–
α	–	–	–	30º	30º	30º	–	–	–
d (m)	–	–	–	0.05	0.05	0.05	–	–	–
Radius (m), nbpoints	–	–	–	–	–	–	3.0; 10	3.0; 10	3.0; 5

3 Proposed Method

The proposed method consists of (1) extracting candidate ground points using KDE, (2) filtering ground points using PCA, and (3) generating DEM (Fig. 2).

Step 1: Candidate ground points extraction

The proposed method first decomposes the point clouds into 2D cell grids in the xy plane. The points within a cell are determined based on the coordinates of the cell's bottom left and upright corners. Next, a distribution of the point elevations in each cell is investigated using kernel density estimation (KDE). The resulting local peaks of a KDE distribution enable the classification of the points within the cell as ground and non-ground points. The points within the lowest local peak are presumed to be the ground point. Cell sizes are selected to be larger than tree canopies or building surfaces to prevent cells from solely consisting of non-ground points.

In Step 1, three important parameters must be defined: cell size (cs), bandwidth (bw), and the number of locations of KDE. A cell size determines an object's maximum length, typically with an additional 2–5 m margin. The bandwidth of KDE depends on the slope and terrain distribution, in which the small bandwidth is used for the smooth surface and vice-versa. The value of the bandwidth significantly affects processing speed and the quality of candidate ground point extraction. The number of sampling points of KDE is used to estimate the potential ground plane. A suitable, more significant number of

sampling points can estimate the ground plane accurately, but the processing time was increased. A 5cm or 10cm range is often the optimal choice for UAV image-generated point cloud data.

Step 2: Ground points extraction

Step 1 classified the point clouds into the non- and candidate-ground points. However, the candidate ground point may still contain non-ground points filtered in this step. First, the cell grid was re-created from the set of the candidate ground points with a cell size of 2.0 m. For each cell, PCA was employed to estimate eigenvalues and eigenvectors, in which the points within the cell are assumed to describe a plane (Eq. 1).

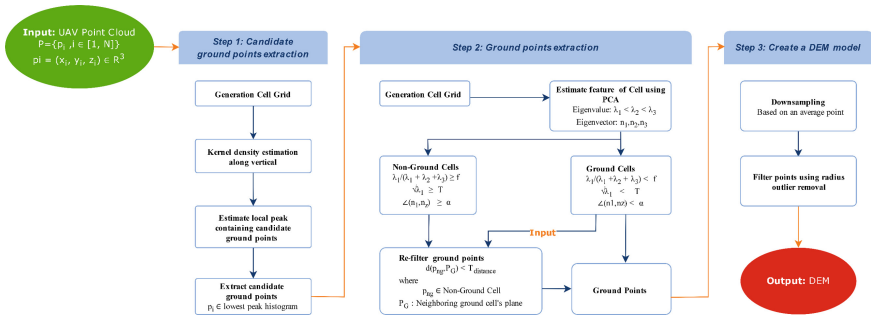$$Plane : a(x - x_0) + b(y - y_0) + c(z - z_0) = 0 \tag{1}$$

Fig. 2. The proposed method involves the extraction of ground points and the generation of a DEM.

In addition, a cell was classified as a ground or non-ground cell if features derived from the eigenvalues and eigenvectors satisfy (Eqs. 2–4):

$$C = \frac{\lambda_1}{\lambda_1 + \lambda_2 + \lambda_3} < f \tag{2}$$

$$S = \sqrt{\lambda_1} < T \tag{3}$$

$$A = \widehat{(n_1, n_z)} < \alpha \tag{4}$$

where: $\lambda_1 > \lambda_2 > \lambda_3$ are the eigenvalues of each cell.

n_1 is the eigenvector corresponding to λ_1.

n_z is the unit vector of the oz axis.

As cell-based filtering was used to eliminate non-ground points, non-ground cells may contain ground points, which were re-extracted. Based on observation, the ground points within the non-ground cell are co-plane with the points within the adjacent ground cells. The points within the non-ground cell were considered the ground point if the

distance (d) from these points to the fitting plane obtained from the points within adjacent ground cells of the non-ground cell satisfied Eq. (5). Notably, PCA was used to estimate the fitting plane.
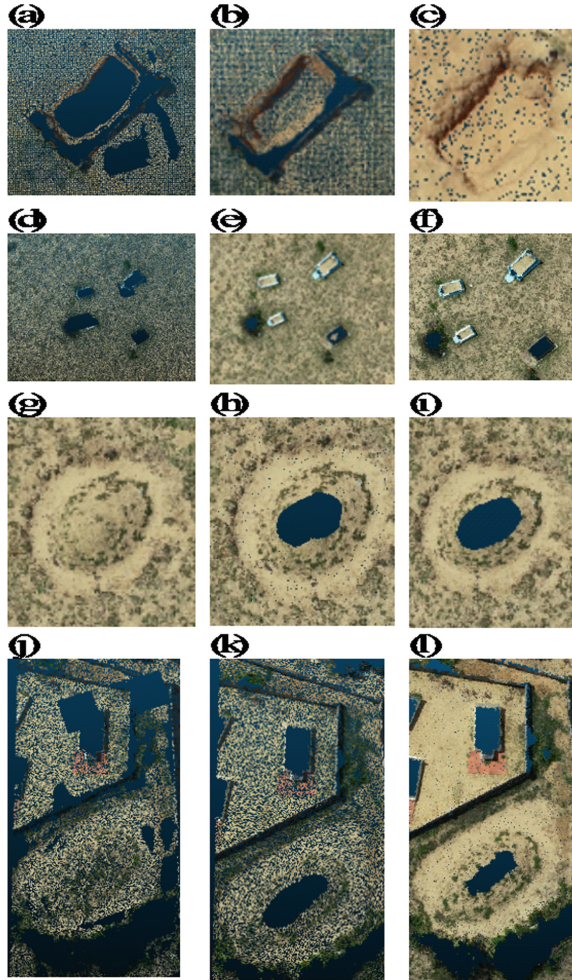
$$d(p_{NG}, P_G) < d \tag{5}$$

Fig. 3. There are differences in the locations extracted by different methods in Test 3 dataset. Columns imply the results of (**a, d, g, j**) proposed method, (**b, e, h, k**) CSF, and (**c, f, i, l**) Classify Ground Points (Agisoft Metashape)

where: p_{NG} is points in non-ground cells.

P_G is the fitting plane estimated from points within the neighboring ground cells.
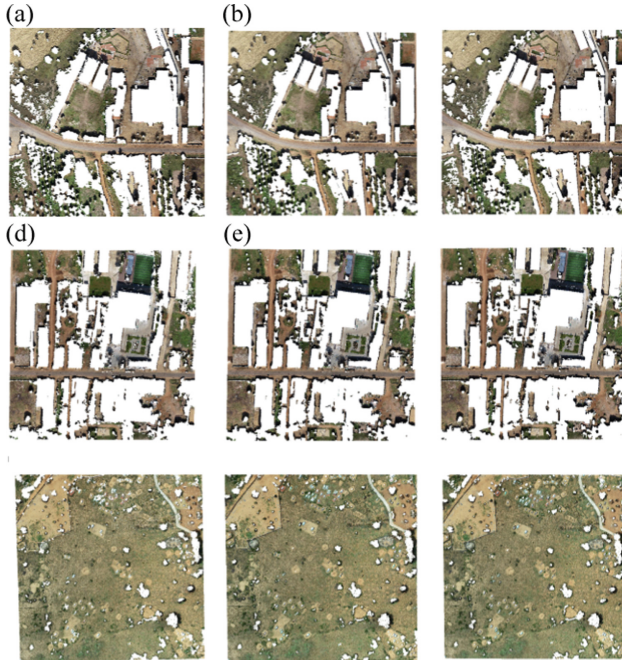
Fig. 4. The ground point extracted by different methods. Columns imply the results of (**a**, **d**, **g**) proposed method, (**b**, **e**, **h**) CSF, and (**c**, **f**, **i**) Classify Ground Points (Agisoft Metashape). Rows imply the results of test site 1 (**a–c**), test site 2 (**d–f**) and test site 3 (**g–i**)
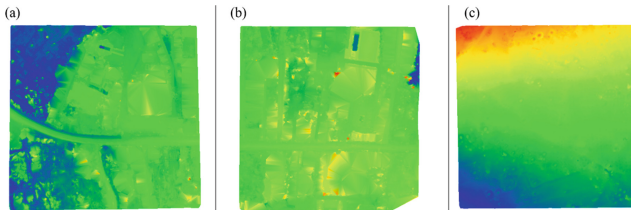

Fig. 5. The results of the DEM model are generated by the proposed method. **a** Site 1, **b** site 2, and **c** site 3

Step 2 keeps the parameters cs, f, and T constant. α represents the threshold angle and depends on the slope of the terrain. The d parameter, on the other hand, depends on the user's desired level of accuracy of results.

Step 3: Creating a digital elevation model

The spatial resolution of DEM is set to 1.0 m. From the ground points extracted in Step 2, a representative point in each cell is computed based on the average points within the cell. Then, a Radius Outlier Removal method was used to eliminate outlier points from the set of representative points. Finally, DEM was created using the Delaunay triangulation method.
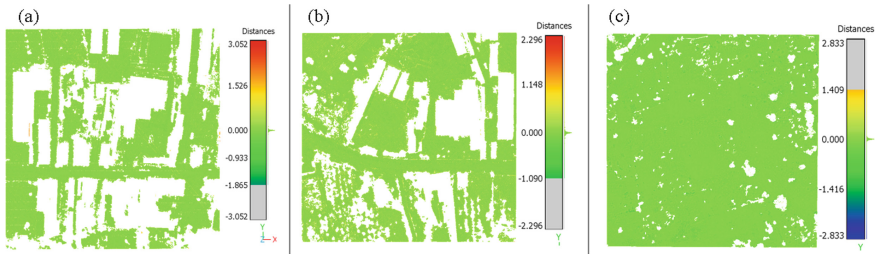
Fig. 6. The difference in height between generated DEM and ground surface

In this step, three main parameters are considered. First, the cell size represents DEM resolution. The other (radius and nbpoints) depend on the data noise level. The radius parameter specifies the distance for searching neighbors surrounding the evaluated target point, whereas the nbpoints parameter sets the minimum number of points required within the specified radius. These two parameters help determine the criteria for identifying and removing outliers in the data.

4   Results and Discussion

Each dataset has different characteristics and on-ground object components, so the parameters were adjusted to represent them appropriately. The value of setting parameters for each test site is displayed in Table 2.

Following Step 1 and Step 2, the ground point data has been obtained (Figs. 3, 4). The accuracy of ground point extraction is checked by comparing the ground data derived by the proposed method and other results accepted using the CSF algorithm (with the Flat parameter) and utilizing the Classify Ground Points function in Agisoft Metashape (employing parameters surveyed on Google Earth Pro). Figure 3 show that the proposed and two other mentioned method incorrectly removes specific ground points in localized areas with steep slopes. These observations indicate that none of the three methods has achieved perfect accuracy in ground point filtering. However, the proposed method achieved good results for the test site with many on-ground objects and a slight slope angle.

According to the result, most non-ground points have been removed (Fig. 4). Several non-ground issues exist, such as the building points closing to the ground surface. They will be released in the final step of creating DEM. Figure 4 shows that the proposed algorithm outperforms the other two methods in ground point filtering in Test site 1 and Test site 2 (Fig. 4a, d), whereas, in Test site 3 (Fig. 4g), the CSF algorithm achieves the best results, despite still having some non-ground points (Fig. 4h). On the other hand, the ground point the proposed method extracts will become the input value for generating DEM.

In the final step, the data is divided into cells with a size of 1.0 m, and the average method is used to sample the data within each cell. This step aims to obtain a representative set of points that accurately capture the ground surface. To achieve this, the Radius Outlier Removal algorithm is applied to filter out noisy points that may result in

misclassification. By eliminating these outliers, the algorithm ensures that the selected points best represent the ground surface. Following the outlier removal, the Delaunay triangulation technique is utilized to create a triangular network, which forms the basis for visualizing the Digital Elevation Model (DEM). The resulting DEM model, obtained through the proposed method, is showcased in Fig. 5. This visualization provides a general overview of the target site, allowing us to observe its topography. Specifically, the upper left corner of site 3 exhibits higher elevated land, visually depicted in red. One significant advantage of storing the data as a set of 3D points is the ease with which it can be employed for future analysis and calculations. This format enables straightforward utilization in various analytical tasks, facilitating further investigation and exploration of the dataset.

Moreover, the differences between created DEM and ground points are checked to ensure that DEM is well represented for the ground surface. The process was done with the CloudCompare application. The comparison result provides insights into the accuracy and quality of the generated DEM. The visual comparison results are presented in Fig. 6. Negligible deviations are observed between the ground point cloud and the developed numerical elevation model (DEM), except for a few points where variations occur due to the complexities involved in removing non-ground points. The average deviations between the ground point cloud and the DEM are 5.38 mm, 13.53 mm, and 15.67 mm for Test sites 1, 2, and 3, respectively. This result implies a good match between generated DEM and the ground surface, whereas the absolute accuracy developed from UAV images is approximately 7.0 cm [14].

5   Conclusion

This study proposed an automatic method for generating a DEM model from point clouds generated from UAV images, which consists of three steps: ground point and non-ground point classification based on geometric characteristics of the ground and computing the value of the representative points for creating a DEM model and visualizing DEM using Delaunay triangulation. The proposed method was tested on 2 Areas covering about 45 ha, in which average deviations between the ground point cloud (the ground truth) and DEMs are 5.38 mm, 13.53 mm, and 15.67 mm for Test site 1, Test site 2, and Test site 3, respectively. That implied the proposed method's ability to generate DEM from the point cloud created from a UAV-images. Visualization check also sees extracted ground points consistent with results from two CFS and Classify Ground Points (Agisoft Metashape). Moreover, the cell-based analysis approach implemented in the proposed method has difficulty extracting the ground points where the elevation surface change rapidly, which causes under-extraction of the ground points. This problem was also found in other methods.

References

1. Gómez-Reyes JK, Benítez-Rangel JP, Morales-Hernández LA, Resendiz-Ochoa E, Camarillo-Gomez KA (2022) Image Mosaicing Applied on UAVs Survey. Appl Sci 12:2729. https://doi.org/10.3390/app12052729
2. Sun J, Peng B, Wang C, Chen K, Zhong B, Wu J (2022) Building displacement measurement and analysis based on UAV images. Autom Constr 140(2022):104367. https://doi.org/10.1016/j.autcon.2022.104367
3. Zhu J, Zhong J, Ma T, Huang X, Zhang W, Zhou W (2022) Pavement distress detection using convolutional neural networks with images captured via UAV. Autom Constr 133. https://doi.org/10.1016/j.autcon.2021.103991
4. Voroninski V, Basri R, Singer A (2017) A survey of structure from motion. Acta Numerica, pp 305–364
5. Zhang W et al (2016) An Easy-to-Use Airborne LiDAR Data Filtering Method Based on Cloth Simulation. Remote Sens 8(6):501
6. Evans J, Hudak A (2007) A multiscale curvature algorithm for classifying discrete return LiDAR in forested environments. IEEE Trans Geosci Remote Sens 45(4):1029–1038
7. Zhao X, Guo Q, Su Y, Xue B (2016) Improved progressive TIN densification filtering algorithm for airborne LiDAR data in forested areas. ISPRS J Photogramm Remote Sens 117:79–91
8. Hu H et al (2014) An adaptive surface filter for airborne laser scanning point clouds by means of regularization and bending energy. ISPRS J Photogramm Remote Sens 92:98–111
9. Hu X, Yuan Y (2016) (**2016**) Deep-Learning-Based Classification for DTM Extraction from ALS Point Cloud. Remote Sens 8:730
10. Kang Y, Noh Y, Lim O (2017) Kernel density estimation with bounded data. Struct Multidiscip Optim 57:95–113
11. Karamizadeh S, Abdullah S, Manaf A, Zamani M, Hooman A (2013) An Overview of Principal Component Analysis. Journal of Signal and Information Processing 4:173–175
12. Hojjatoleslami SA, Kittler J (1998) Region growing: a new approach. IEEE Trans Image Process 7:1079–1084
13. Gan G, Kwok-Po NM (2017) K-means clustering with outlier removal. Pattern Recogn Lett 90:8–14
14. Uysal M, Toprak AS, Polat N (2015) DEM generation with UAV Photogrammetry and accuracy analysis in Sahitler hill. Measurement 73:539–543. https://doi.org/10.1016/j.measurement.2015.06.010